Magnetic tailoring of the nature of the fundamental optical transition in a ZnSe/(Zn,Mn)Se heterostructure

E. Deleporte, T. Lebihen, B. Ohnesorge, Ph. Roussignol, and C. Delalande
Laboratoire de Physique de la Matière Condensée de l'Ecole Normale Supérieure, 24 rue Lhomond, 75005 Paris, France

S. Guha* and H. Munekata
IBM Research Division, Thomas J. Watson Research Center, P. O. Box 218, Yorktown Heights, New York 10598
(Received 19 January 1994)

We report on optical measurements performed on two 53 and 106 Å wide ZnSe quantum wells separated by a 350-Å-thick $Zn_{0.73}Mn_{0.27}Se$ barrier. The measurements were done by means of cw photoluminescence, cw photoluminescence excitation, and time-resolved photoluminescence spectroscopies at low temperature and under a magnetic field up to 5.5 T. They allow us to determine the strain state of the different layers and the valence-band offset between the ternary and binary alloys. Moreover magnetic tailoring of the nature of the fundamental optical transition from a type-I light-hole exciton to a type-II heavy-hole exciton is evidenced. Calculations taking into account the strain, Zeeman, and excitonic effects are presented and support the experimental findings.

I. INTRODUCTION

Among the various II-VI compounds, the ZnSe-based materials are particularly interesting because of their blue emission. The first blue laser emission was obtained with ZeSe-based compounds.[1] Among II-VI wide-gap materials, semimagnetic heterostructures like ZnSe/(Zn,Mn)Se or ZnSe/(Zn,Fe)Se are of particular interest because of their remarkable magneto-optical properties, due to the exchange interaction between the spin of the carriers and the spin of the paramagnetic Mn^{2+} or Fe^{2+} ions located in ternary alloy layers.[2,3] The application of an external magnetic field at low temperature, inducing the so-called giant Zeemann effect of the band edges, gives rise to the possibility of magnetic tuning of the barrier heights experienced by the carriers. In particular, the giant Zeeman effect can lead to the formation of a spin superlattice structure in which the carriers can be separated and spatially localized according to their spin.[3,4]

In this paper we show that, in a ZnSe/(Zn,Mn)Se heterostructure, it is possible to change the nature of the fundamental optical transition from a type-I light-hole exciton to a type-II heavy-hole exciton by tuning the applied magnetic field.

In Sec. II we will report on experimental results obtained for a $ZnSe/Zn_{0.73}Mn_{0.27}Se$ heterostructure by means of optical techniques: cw photoluminescence and photoluminescence excitation spectroscopy, and time-resolved photoluminescence spectroscopy. All measurements were performed at low temperature ($T \leq 10$ K) and under a magnetic field up to 5.5 T. In Sec. III we present calculations performed in order to interpret the experimental findings: the energy of the different optical transitions is obtained, taking into account the strain effects, the giant Zeeman effect, and the excitonic effect on the band structure. In Sec. IV, a comparison between theory and experiment is done. This comparison allows us to specify the band structure of our heterostructure; we can estimate some relevant parameters, such as the strain state of the different layers and the valence-band offset between ternary and binary alloys. Moreover, we can ascertain the magnetic tailoring of the nature of the fundamental optical transition, from a type-I light-hole exciton to a type-II heavy-hole exciton.

II. EXPERIMENTAL RESULTS

A. Sample and experimental setup

The heterostructure has been grown by molecular-beam epitaxy along the (100) axis on a GaAs substrate. It consists in two 53- and 106-Å ZnSe quantum wells, separated by a 350-Å-thick $Zn_{0.73}Mn_{0.27}Se$ layer. The double quantum well is grown on a 1200-Å $Zn_{0.73}Mn_{0.27}Se$ layer deposited on a 9700-Å-thick ZnSe buffer layer. The cap layer consists in a 350-Å $Zn_{0.73}Mn_{0.27}Se$ layer.

This heterostructure was investigated by means of cw and time-resolved optical experiments at low temperatures (1.7, 4.2, and 10 K). Additionally, magnetic fields up to 5.5 T were applied by a superconducting magnet in order to perform magneto-optical experiments in the Faraday configuration. The excitation source for cw photoluminescence experiments was the 363-nm line of an Ar^+ laser. In photoluminescence excitation and time-resolved spectroscopy, excitation was provided by a mode-locked and frequency-doubled Ti-Sa laser, producing 2-ps pulses with a 82-MHz repetition rate in the 4200–4500-Å range. A multifiber optical guide was used to send the excitation light to the sample and to collect the outgoing photoluminescence signal. The photoluminescence signal was then analyzed by a double Jobin-Yvon $f=25$ cm monochromator with a spectral resolution of about 1 meV. The detection was provided by a synchroscan streak camera. In excitation spectroscopy measurements time-integrated spectra were record-

ed when in time-resolved photoluminescence measurements the overall temporal solution was about 15 ps. The excitation power, taking into account the absorption losses in the optical fiber, was 30 mW, corresponding to an excitation density of 10^{15} cm^{-3}.

B. cw experiments

1. Zero magnetic field

Figure 1 shows the photoluminescence spectrum of the heterostructure at zero magnetic field. Four lines with widely different intensities are observed. The two strong lines labeled PL_W(2.773 eV) and PL_T (2.808 eV) correspond to the excitonic recombination of the wide and thin wells, respectively. The other two lines are much weaker. The energy position of the 2942-meV one (PL_B) is coherent with the value of the band gap of a $Zn_{0.73}Mn_{0.27}Se$ layer.[5,6] We will comment below on the nature of the 2830-meV one (PL'_T).

The excitation spectra (SE_W) and (SE_T) of the PL_W and PL_T lines, respectively, are shown in Fig. 2. SE_W is performed at the detection energy 2.764 eV and SE_T at 2.795 eV. Each excitation spectrum exhibits two excitonic lines confirming the bidimensional character of the density of states: the fundamental excitonic transitions X^W_{LH} and X^T_{LH} and the first excitation transitions X^W_{HH} and X^T_{HH} for the wide and thin wells, respectively. We remark first that the Stokes shifts between the photoluminescence lines and the first lines of the corresponding excitation spectra (6 meV for the thin well and 2 meV for the wide well) are small, indicating the good quality of the heterostructure. The two wells are clearly uncoupled,

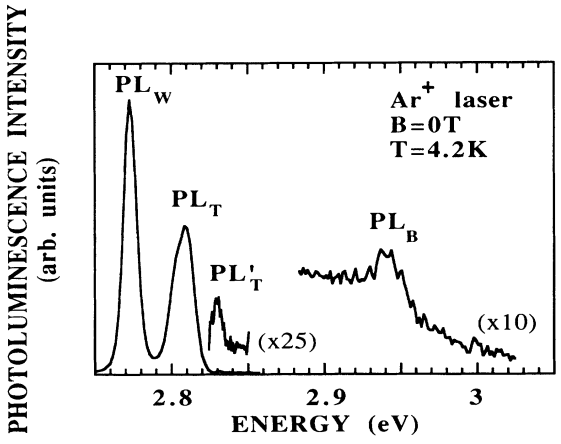

FIG. 1. Photoluminescence spectrum of the heterostructure, performed with the 363-nm line of an Ar^+ laser, at zero magnetic field and low temperature T=4.2 K. PL_W, PL_T, and PL_B lines are associated with the excitonic recombinations in the wide quantum well, the thin quantum well, and the $Zn_{0.73}Mn_{0.27}Se$ barriers, respectively. The PL'_T line is associated with an excited optical transition of the thin well.

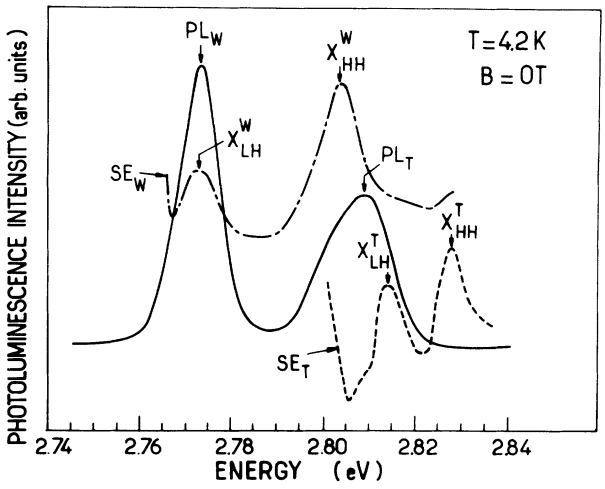

FIG. 2. Photoluminescence (full line) and photoluminescence excitation spectroscopy SE_W and SE_T of the 106-Å and 53-Å quantum wells, respectively, at zero magnetic field and low temperature (4.2 K). SE_W (dashed-dotted line) was performed at E_{det}=2.764 eV and SE_T (dashed line) at E_{det}=2.795 eV.

the two excitation spectra (SE_W) and (SE_T) being independent. They will be treated in this paper as single quantum wells. Moreover, the PL'_T line lies at the same energy as X^T_{HH}, which is the first excited transition of the thin well. The PL'_T line is actually an excited transition in the photoluminescence spectrum, which is observed because of the electronic temperature caused by a strong excitation power.

2. Nonzero magnetic field

In fact, we expect the excitonic transition energies to be largely affected by the magnetic field due to the existence of the giant Zeeman effect in the $Zn_{0.73}Mn_{0.27}Se$ layers.[2] Thus we have applied a magnetic field parallel to the growth axis of the heterostructure (Faraday configuration). The temperature was kept at 4.2 K. Figure 3 shows the variation of the four aforementioned photoluminescence lines as a function of the magnetic field. The redshift of the barrier photoluminescence PL_B [Fig. 3(a)] is very large: 30 meV for 5.5 T. This value is consistent with the large redshift of the optical fundamental heavy-hole transition usually observed in a semimagnetic (Zn,Mn)Se layer.[2,7] The PL_W line [Fig. 3(d)] does not move at all with the magnetic field and the PL_T line [Fig. 3(c)] exhibits a small redshift, 7 meV for 5.5 T. Finally, the PL'_T line [Fig. 3(b)] is seen only up to 1.5 T and, when observable, its redshift is quite parallel to the PL_B redshift.

Figure 4 shows the evolution of the excitation spectra of the thin well [Fig. 4(a)] and wide well [Fig. 4(b)] for different magnetic fields. The Zeeman splitting of the X^W_{HH} and X^T_{HH} lines into two components σ^+ and σ^- is large. On the contrary, the Zeeman splitting of the X^W_{LH} and X^T_{LH} lines is too small (less than 1 meV for 6 T, see

Sec. IV) to be resolved in these spectra due to the large spectral width of the lines (more than 5 meV). The small Zeeman splitting of the X^W_{LH} and X^T_{LH} lines is an indication of the light-hole character of the fundamental excitonic transition in the two wells, at least at low magnetic field; the large Zeeman splitting of the X^W_{HH} and X^T_{HH} lines indicates the heavy-hole character of the first excited optical transition in the two wells.[2,8]

Note also that the variation with the magnetic field of the transition energies of the X^W_{HH} and $X^T_{HH}\sigma^-$ components is smaller than the one of the σ^+ components. The behavior of the σ^+ component of X^T_{HH} in Fig. 4(a) is particularly noticeable. When the magnetic field increases, this component is strongly redshifted, while the energy of the X^T_{LH} line is practically independent of the magnetic field. Thus these two lines approach each other. For $2<B<3.5$ T, the large width of the lines does not allow us to distinguish the two peaks. But at high magnetic field ($B=5.5$ T), two peaks can be resolved again: the X^T_{LH} and $X^T_{HH}(\sigma^+)$ lines have crossed each other. Such a crossing is not observed in the excitation spectrum of the wide well [Fig. 4(b)] in this magnetic-field range.

C. Time-resolved experiments

Time-resolved photoluminescence spectroscopy allowed us to study the recombination time of the carriers in the thin and wide wells, as a function of the magnetic field for different temperatures (1.7, 4.2, and 10 K).

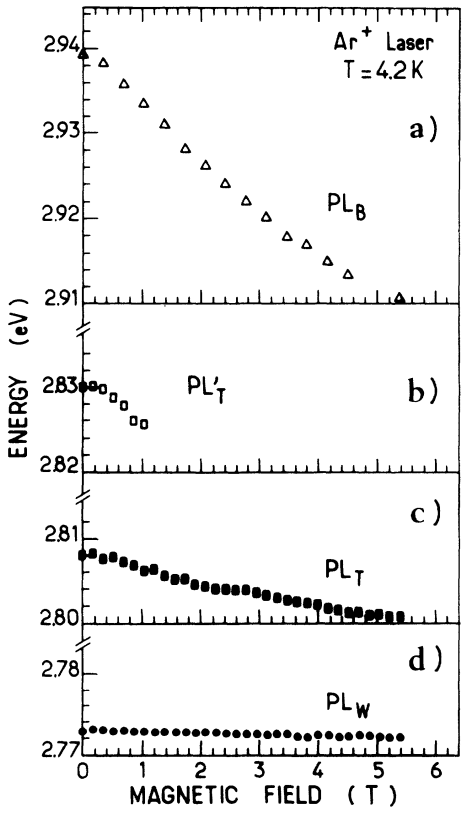

FIG. 3. Magnetic-field-induced variation of the four observed photoluminescence lines of Fig. 1, up to 5.5 T, at low temperature $T=4.2$ K: (a) barrier photoluminescence PL_B, (b) PL'_T line corresponding to the first excited optical transition of the thin well, (c) photoluminescence of the thin well PL_T, and (d) photoluminescence of the wide well PL_w.

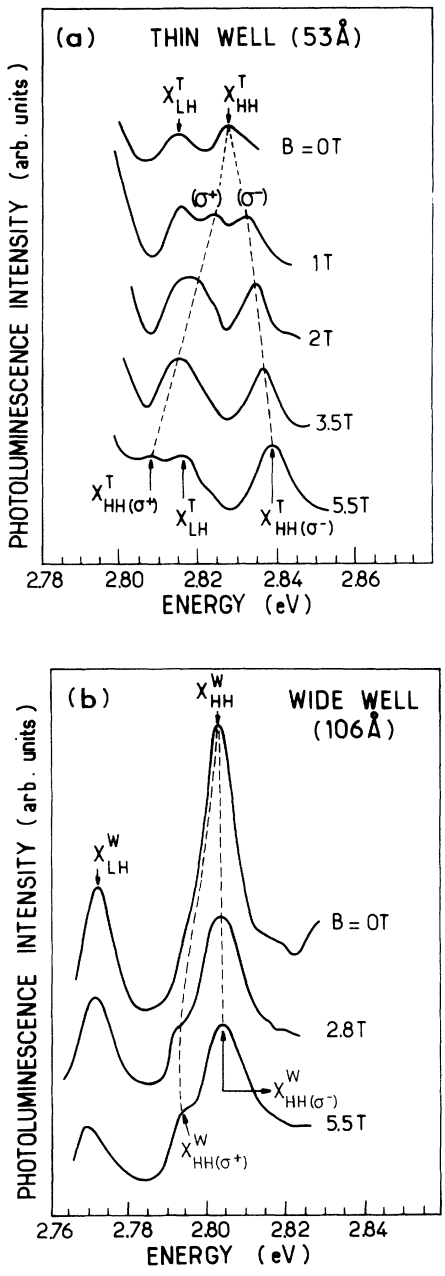

FIG. 4. Evolution of the excitation spectra of the 53-Å thin well [(a) $E_{det}=2.794$ eV], and of the 106-Å wide well [(b) $E_{det}=2.764$ eV] for different magnetic fields, at low temperature (4.2 K).

In time-resolved experiments, the heterostructure was excited well above the (Zn,Mn)Se gap energy, at 3.379 eV. This excitation preferentially creates carriers in the barrier layers. The recorded emission profiles were fitted by appropriately choosing an effective relaxation time τ_{eff} and an overall recombination time τ. τ_{eff} takes into account the carrier capture from the barrier layers into a quantum well and the relaxation to the fundamental subband. Excitonic recombination can be either radiative or nonradiative with characteristic times τ_R and τ_{NR}, respectively, so that

$$\frac{1}{\tau}=\frac{1}{\tau_R}+\frac{1}{\tau_{\text{NR}}} . \tag{1}$$

Due to the time scales involved here, the effective relaxation time τ_{eff} determines the rise of the profiles, while the photoluminescence decay is given above all by the recombination time τ. Furthermore the profile analysis took into account the finite resolution time of our experimental setup (pulse duration plus spectrometer plus streak camera).

Typical time-resolved photoluminescence spectra of the thin well (line PL_T) are shown in Fig. 5 for two values of the magnetic field at low temperature (1.7 K). The rise times are found to be very short (τ_{eff}=10–20 ps), and the decay can be well fitted by a single exponential with recombination times ranging from 110 ps for low magnetic fields to 240 ps for high magnetic fields.

The determination of the recombination time requires a great deal of caution because of the relatively wide and inhomogeneous photoluminescence lines. For example, in Fig. 6 we report the cw photoluminescence line of the thin well at B=0 T and T=1.7 K, whose full width at half maximum is 17 meV, and the recombination times obtained when the detection energy scans this line. On the low-energy side, localized excitons bound to impurities may account for a decrease in recombination time, while carriers generated at the high-energy side of the photoluminescence line possess two channels of relaxation–intersubband and intrasubband relaxation

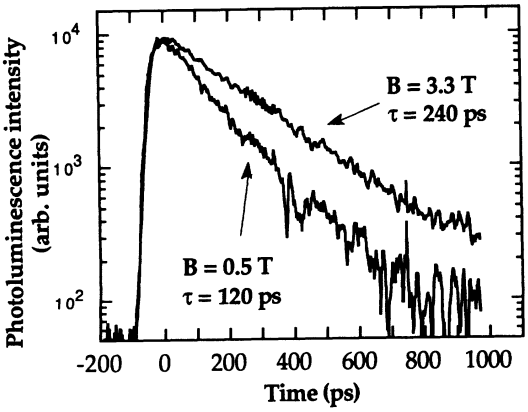

FIG. 5. Typical time-resolved luminescence spectra of the thin well at T=1.7 K for two values of the magnetic field: B=0.5 and 3.3 T.

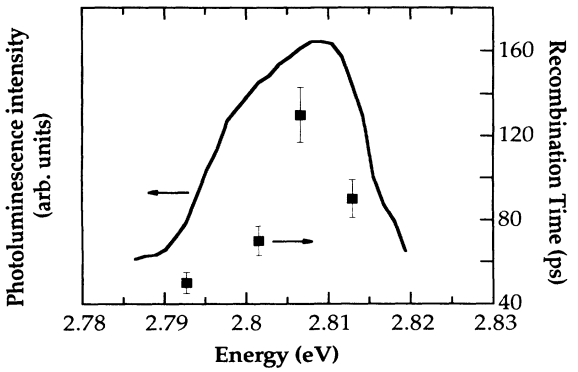

FIG. 6. Photoluminescence line of the thin well at B=0 T and T=1.7 K, and recombination times (squares) measured at the corresponding detection energy and reported with their uncertainty.

(the excitation power is large)—thereby decreasing the lifetime as well. It has been noted in our sample that the maximal of value of τ is obtained when the detection energy corresponds to the maximum of the cw photoluminescence line. Thus, in order to be able to compare the recombination times for different magnetic fields, we were very careful to detect systematically the time-resolved photoluminescence signal at an energy corresponding to the maximum of the cw line.

Figure 7 exhibits a variation of the recombination time

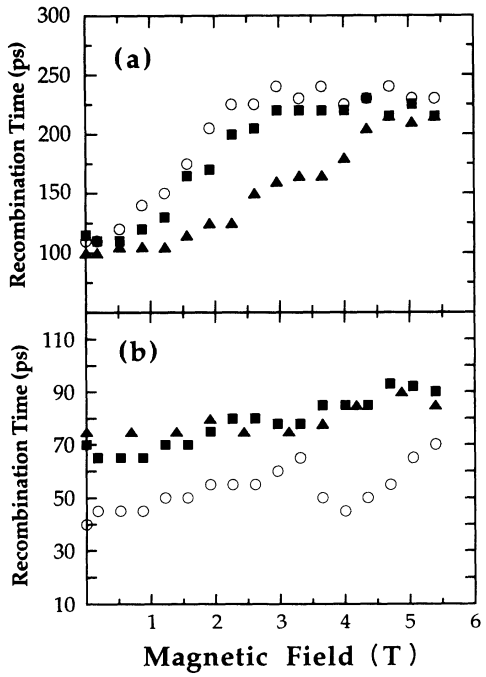

FIG. 7. Recombination time as a function of the magnetic field for three different temperatures; T=1.7 (dots), 4.2 (squares), and 10 K (triangles) for the luminescence of (a) the thin well and (b) the wide well.

τ^T in the thin well [Fig. 7(a)] and τ^W in the wide well [Fig. 7(b)] versus the magnetic field for three different temperatures: 1.7, 4.2, and 10 K. A great difference in the behavior of the recombination times of the thin and wide wells is observed. When the magnetic field is increased from 0 to 2.5 T, the recombination time of the thin well τ^T at $T=1.7$ and 4.2 K rises by a factor of about 2 (from 110 to 240 ps), slightly slower in the latter case. From $B=2.5$ T onwards they remain constant. For $T=10$ K, τ^T grows much more slowly, reaching a plateau only at $B=4.5$ T. In contrast, the recombination time in the wide well τ^W increases much less markedly than τ^T versus the magnetic field for the three temperatures (τ^W at $B=5.5$ T is only 20% larger than τ^W at $B=0$ T).

Furthermore, time-resolved resonant measurements have been performed for several magnetic fields by exciting the heterostructure resonantly with the energy of the fundamental and first excited optical transitions observed in the cw excitation spectra [X^T_{LH} or $X^T_{\mathrm{HH}}(\sigma^+)$ and X^W_{LH}]. As in the time-resolved experiment described above, the detection energy is set to the maximum of the photoluminescence line. For both wells, we found equally short rise times (10–20 ps) and a similar behavior of the recombination times as a function of magnetic field, as in the nonresonant experiment described above. We therefore conclude that the process of carrier collection from barriers in the wells[9] situated only 350 Å apart from the sample surface does not considerably influence our time-resolved spectra.

III. THEORY

In this section we present a theoretical calculation of the transition energies of our ZnSe/(Zn,Mn)Se heterostructure. Strain effects resulting from the lattice mismatch between the binary and ternary alloys, the Zeeman effect, the excitonic effects, and the diamagnetism of the exciton are taken into account.

A. Strain effects

Because of the great lattice mismatch between the binary and ternary alloys, large strains are present in the structure and strongly modify the potential profile along the growth axis (z axis) through the strain Hamiltonian.[10] In fact, the strain effect produces shifts of the conduction and valence-band extrema in each strained layer, which for a $\langle 001 \rangle$ heterostructure[11,5] are

$$\begin{aligned}
\Delta_\varepsilon E_c &= -S\varepsilon a_c \ , \\
\Delta_\varepsilon E_{\mathrm{hh}} &= -S\varepsilon a_v + S'\varepsilon b_v \ , \\
\Delta_\varepsilon E_{\mathrm{lh}} &= -S\varepsilon a_v - S'\varepsilon b_v \ ,
\end{aligned} \tag{2}$$

where

$$\begin{aligned}
S &= \frac{2(S_{11}+2S_{12})}{S_{11}+S_{12}} \ , \\
S' &= \frac{S_{11}-S_{12}}{S_{11}+S_{12}} \ .
\end{aligned} \tag{3}$$

$b_V=-1.2$ eV, $a_c-a_v=5.4$ eV,[12] and $a_v=-1.4$ eV (Ref. 13) are the deformation potentials of ZnSe, and $S_{11}=2.26.10^{-11}$ m^{2}N^{-1} and $S_{12}=-0.85.10^{-11}$ m^{2}N^{-1} are the ZnSe elastic constants.[14] The deformation potentials and the elastic constants in (Zn,Mn)Se layers are taken to be the same as in ZnSe ones. ε is the relative mismatch of the considered layer $\varepsilon=(a-a^0)/a$, where a is the parameter of the whole strained structure and a^0 the strain-free lattice constant [$a^0=5.666$ Å for ZnSe and $5.666+0.268x$ Å for $Zn_{1-x}Mn_xSe$ (Ref. 15)].

From Eqs. (2) and (3) we deduce that the energy-gap variation is

$$\begin{aligned}
&\Delta_\varepsilon E_c - \Delta_\varepsilon E_{\mathrm{hh}} = -1.64\varepsilon \text{ eV for the heavy holes} \\
&\Delta_\varepsilon E_c - \Delta_\varepsilon E_{\mathrm{lh}} = -6.94\varepsilon \text{ eV for the light holes} \ .
\end{aligned} \tag{4}$$

Thus the energy gap of a compressed layer increases, and the increase is much larger for light-hole transitions than for heavy-hole transitions.

B. Zeeman effect

In bulk $Zn_{1-x}Mn_xSe$, when a magnetic field parallel to the growth axis is applied, the shift of an electron state due to the exchange interaction between the Mn^{2+} ions and carrier spins is given by[2]

$$\Delta_B E_c(J_z) = J_z N_0 \alpha x \langle S_z \rangle \ . \tag{5}$$

The corresponding term for the valence band reads

$$\Delta_B E_v(J_z) = J_z \frac{N_0\beta}{3} x \langle S_z \rangle \ . \tag{6}$$

$\langle S_Z \rangle$ is the thermal average of the z component of the Mn^{2+} spin, which involves a Brillouin-like function $B_{5/2}$ depending on the magnetic field and the temperature:

$$\langle S_z \rangle = -S_0 B_{5/2}\left[\frac{\frac{5}{2}g\mu_B B}{k_B(T+T_0)}\right] \ , \tag{7}$$

where $g=2$, μ_B, and k_B are the Landé g factor, Bohr magneton, and Boltzmann constant, respectively. S_0 and T_0 are phenomenological parameters which take into account the antiferromagnetic interaction between the Mn^{2+} ions.

J_z is the component of the angular momentum along the z direction ($J_z=\pm\frac{1}{2}$ for electrons, and $\pm\frac{3}{2}$ and $\pm\frac{1}{2}$ for heavy and light holes, respectively). N_0 is the number of unit cells per unit volume, α and β the exchange integrals [we have taken the experimental values $N_0\alpha=0.29$ eV and $N_0\beta=-1.4$ eV (Ref. 2)]. Note that the exchange interaction is much stronger for the valence band than for the conduction band, and three times stronger for the heavy holes than for the light holes. The effect of the magnetic field on the band structure is then to decrease (increase) the energy gap of $Zn_{1-x}Mn_xSe$ for transitions involving holes with a negative (positive) angular momentum, that is to say for the σ^+ (σ^-) transitions.

To calculate the effect of magnetic field on the potential profile, we neglect the Zeeman splitting in the nonmagnetic layer ZnSe, compared with the giant Zeemann

effect in (Zn,Mn)Se layers. Moreover, it has been proved that the Landau quantization can be neglected in our system for the range of applied magnetic fields.

C. Excitonic effects

Because of the large strain effects[16] and large Zeeman effect[17] on the valence-band structure, the band alignment of our heterostructure can become type II, that is, to say electrons are localized in the ZnSe layers and holes in the (Zn,Mn)Se layers. The Coulombic interaction being very different for type-I or type-II structures, a precise knowledge of the excitonic effects is necessary to understand the experimental results.

We have calculated the exciton binding energy by a variational method, detailed in Ref. 18. We assumed that the electron longitudinal motion is unaffected by the Coulombic interaction. On the contrary, the valence-band offset can be very small and even negative in the case of a type-II structure, and the hole wave function is calculated in an effective potential profile averaged on the electronic motion. When a magnetic field is applied, the diamagnetic shift of the exciton is taken into account, and is estimated using first-order perturbation theory.[18]

We have taken 9.25 (Ref. 19) for the relative dielectric constant and $E_X^{3D}=19$ meV for the three-dimensional exciton binding energy in bulk ZnSe. The effective masses along the z direction are $m_e=0.15m_0$, $m_{hh}=0.78m_0$, and $m_{lh}=0.14m_0$ for electron, heavy, and light holes, respectively[20] (the Luttinger parameters deduced from the values of m_{hh} and m_{lh} are $\gamma_1=4.212$ and $\gamma_2=1.465$).

IV. INTERPRETATION

To know completely the band structure of our double quantum well, we have to determine two parameters: the strain state and the potential profile along the growth axis without strain. This potential profile is characterized by the strain-free relative valence-band offset q_v^0, which is the percentage of the band-gap discontinuity between the ternary and binary alloys lying in the valence band. The comparison between cw experimental results at zero magnetic field and the calculation of excitonic transitions can provide knowledge of the strain state, but is not sufficient to determine q_v^0. This parameter will be deduced from the cw magneto-optical experiments.

A. cw experiments

1. Zero magnetic field

Figure 8 confronts experimental results with the calculated excitonic transition energies: X_{LH}^W and X_{HH}^W for the wide well, and X_{LH}^T and X_{HH}^T for the thin well, at $B=0$ T, as a function of the relative mismatch in the (Zn,Mn)Se layers, $\varepsilon_{Zn_{1-x}Mn_xSe}$. The calculations were performed with $q_v^0=10\%$, which is a mean value between all the values found in the literature[21,4] ($0<q_v^0<20\%$). We also assume that the 9700-Å-thick ZnSe buffer layer is completely relaxed on the GaAs substrate.[22] The 1200-Å (Zn,Mn)Se layer, whose thickness is smaller than the critical thickness, is not fully relaxed on the ZnSe buffer layer.[5,23] Then, assuming an elastic accommodation of the ZnSe lattice parameter with the (Zn,Mn)Se one, we can calculate the relative mismatch ε_{ZnSe} of the ZnSe layers. The influence of the strain state on the band structure is then determined using Eqs. (2) and (3). In Fig. 8, note that the light-hole transitions are very sensitive to the value of $\varepsilon_{Zn_{1-x}Mn_xSe}$, contrary to the heavy-hole transitions [see Eq. (4)], and that the nature of the fundamental optical transition depends on the value of ε_{ZnMnSe}. For example, in the thin well, the fundamental excitonic state is a light-hole exciton for $|\varepsilon_{Zn_{1-x}Mn_xSe}|<0.95\%$ and a heavy-hole exciton for $|\varepsilon_{Zn_{1-x}Mn_xSe}|>0.95\%$. The comparison between experimental and calculated results (Fig. 8) explains why the fundamental optical transitions X_{LH}^W and X_{LH}^T are light-hole excitons, while the first excited transitions X_{HH}^W and X_{HH}^T are heavy-hole excitons. Using the fact that the light-hole transition energies are very sensitive to the value of $\varepsilon_{Zn_{1-x}Mn_xSe}$, and comparing the experimental positions of X_{LH}^W and X_{LH}^T (reported in Fig. 8 with their uncertainty) with the calculation, we estimate $\varepsilon_{Zn_{1-x}Mn_xSe}=-0.55\%\pm0.03\%$.

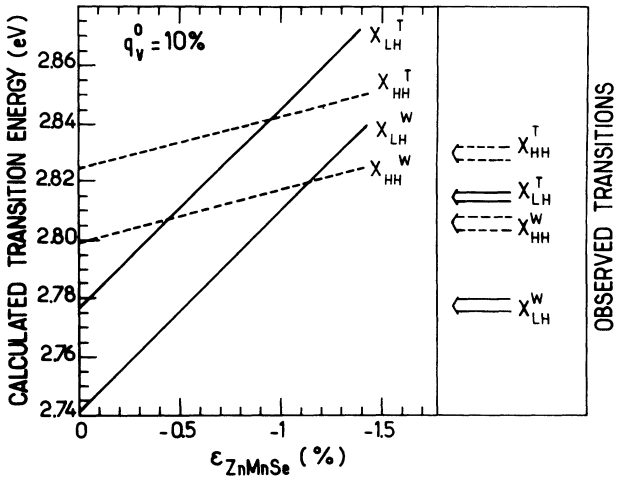

FIG. 8. Calculated energies of the excitonic transitions X_{LH}^W, X_{HH}^W for the wide well, and X_{LH}^T, X_{HH}^T for the thin well, vs the relative mismatch of the (Zn,Mn)Se layer: ε_{ZnMnSe}. We have taken a strain-free relative valence-band offset $q_v^0=10\%$. The arrows correspond to experimental energies which are reported with their uncertainty.

This estimation of $\varepsilon_{Zn_{1-x}Mn_xSe}$ depends *a priori* on the value of q_v^0 taken in the calculation. Thus we have calculated the variation of the excitonic transition energies X_{LH}^W and X_{LH}^T versus the relative valence-band offset q_v^0, as shown in Fig. 9. For the whole q_v^0 range considered in Fig. 9 the light-hole band structure is type I. It is well known that the transition energy of a type-I structure is almost independent of the precise value of q_v^0. Actually, the experimental energy positions of X_{LH}^W and X_{LH}^T, reported in Fig. 9 with their uncertainties, are compatible with the calculated ones for all values of q_v^0 considered

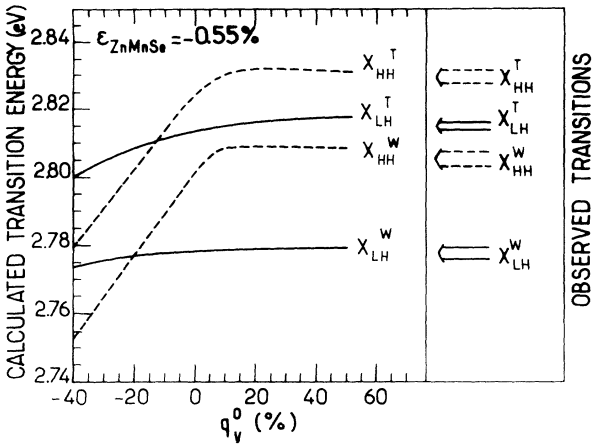

FIG. 9. Calculated energies of the excitonic transitions X_{LH}^W, X_{HH}^W, X_{LH}^T, and X_{HH}^T vs the strain-free relative valence-band offset q_v^0. The relative mismatch of the (Zn,Mn)Se layer: $\varepsilon_{Zn_{1-x}Mn_xSe}$ is taken as $\varepsilon_{Zn_{1-x}Mn_xSe}=-0.55\%$. The arrows correspond to experimental energies which are reported with their uncertainty.

here. Thus our previous estimation of $\varepsilon_{Zn_{1-x}Mn_xSe}$ does not depend on q_v^0.

In Fig. 9 we have also plotted the variation of the excitonic transition energies X_{HH}^W and X_{HH}^T with q_v^0. For $q_v^0 > 15\%$, the band structure of the heavy holes is type I, and the heavy-hole excitonic transition energies are practically constant. On the contrary, for $q_v^0 < 15\%$, due to the strain effects, the heavy-hole transition is type II and the transition energies are very sensitive to q_v^0. The experimental positions of X_{HH}^W and X_{HH}^T are reported in Fig. 9 with their uncertainty. We determine a lower limit for q_v^0 ($q_v^0 > 0\%$), but at this stage it is impossible to determine an upper limit for q_v^0.

2. *Nonzero magnetic field*

Let us first consider the PL_B line. Under magnetic field, its redshift (Fig. 3) behaves like a Brillouin function, and the order of magnitude of the redshift is coherent with the decrease of the σ^+ heavy-hole optical transition energy in (Zn,Mn)Se.[2,7] The optical fundamental transition in the (Zn,Mn)Se layer is thus a heavy-hole exciton, thereby confirming a compressed (Zn,Mn)Se layer [Eq. (4)].

The behavior of the light- and heavy-hole excitonic transitions of the two wells under a magnetic field is quite coherent with earlier findings. The X_{LH}^W and X_{LH}^T transitions are insensitive to the magnetic field, while the Zeeman splitting of the heavy-hole transitions X_{HH}^W and X_{HH}^T is well observed (Fig. 4). The light-hole band structure is type I, and the light-hole wave functions are principally localized in the nonmagnetic ZnSe layers. The interaction between the carriers and Mn^{2+} ion spins is not favored, leading to a small Zeeman splitting. In Fig. 3, note that, in the case of the thin well, due to a larger penetration of the carrier wave function in the barrier, the redshift of the PL_T line (the σ^+ component of X_{LH}^T) is larger than the redshift of the PL_W line (the σ^+ component of X_{LH}^W).

The Zeeman splitting of the X_{HH}^W and X_{HH}^T lines is much larger than the Zeeman splitting of the light-hole transitions (Fig. 4), the exchange interaction being three times larger for the heavy holes than for the light holes. Moreover, the band alignment tends to become type II under a magnetic field for the $-\frac{3}{2}$ component of the heavy holes, as has been found in CdTe/(Cd,Mn)Te heterostructures.[17] When the structure becomes type II, the heavy-hole wave function is principally localized in the (Zn,Mn)Se layers, and the exchange interaction between the carriers spins and the Mn^{2+} spins is enhanced.

In order to understand the particular behavior of the X_{LH}^T and $X_{HH}^T(\sigma^+)$ lines at high magnetic field in the excitation spectrum of the thin well [Fig. 4(a)], we have calculated the energies of the $X_{LH}^T(\sigma^+)$, $X_{LH}^T(\sigma^-)$, $X_{HH}^T(\sigma^+)$, and $X_{HH}^T(\sigma^-)$ excitonic transitions versus the magnetic field for two values of the relative valence-band offset: $q_v^0=5\%$ [Fig. 10(a)] and $q_v^0=20\%$ [Fig. 10(b)].

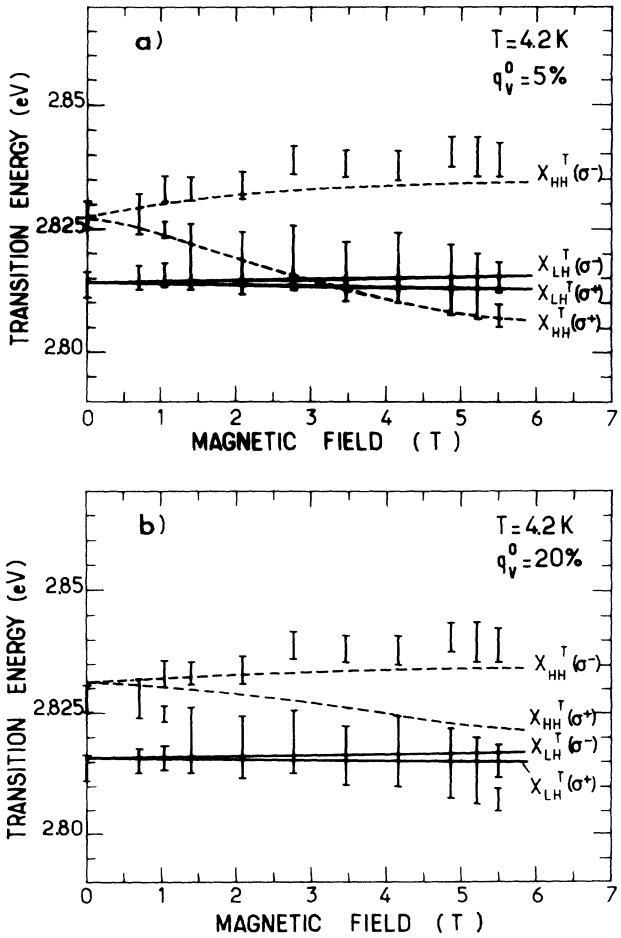

FIG. 10. Energy position of the different lines observed in the excitation spectrum (at low temperature $T=4.2$ K) of the 53-Å thin well and their full width at half maximum (vertical segments) vs the magnetic field. The lines show the calculated excitonic heavy- (dashed line) and light-hole (solid line) transition energies for two values of the strain-free relative valence-band offset: (a) $q_v^0=5\%$, (b) $q_v^0=20\%$.

The band offsets were calculated for each magnetic-field value using the experimental magnetic-field dependence of PL_B [Fig. 3(a)] and Eqs. (5)–(7).

We note the presence of a crossing between the $X^T_{HH}(\sigma^+)$ curve and the $X^T_{LH}(\sigma^+)$ and $X^T_{LH}(\sigma^-)$ curves for $q_v^0=5\%$ at $B=3.3$ and 3 T, respectively [Fig. 10(a)]. In the parabolic model we used for our calculation, the interaction between heavy holes and light holes is not taken into account. As a consequence, a crossing (and not an anticrossing) appears in Fig. 10(a). In Fig. 10 we also reported the energy positions of the different experimental lines $X^T_{LH}(\sigma^+)$, $X^T_{LH}(\sigma^-)$, $X^T_{HH}(\sigma^+)$, and $X^T_{HH}(\sigma^-)$ with their full width at half maximum. In spite of the limited resolution due to the spectral width of the lines, we can note good agreement between the experiment and the calculation for $q_v^0=5\%$, while the calculation for $q_v^0=20\%$ does not reproduce the experimental results at all. Thus the excitation spectrum [Fig. 4(a)] above 4.5 T can easily be interpreted: the fundamental optical transition is the $X^T_{HH}(\sigma^+)$ heavy-hole exciton and the first excited transition is the X^T_{LH} light-hole exciton [$X^T_{LH}(\sigma^+)$ and $X^T_{LH}(\sigma^-)$ merge in the same line, called X^T_{LH}]. Figure 10(a) shows clearly the crossing between the X^T_{LH} and $X^T_{HH}(\sigma^+)$ transitions, and so the existence of a critical magnetic field B_c for which a transition in the nature of the fundamental state occurs: for $B<B_c$, the fundamental optical transition is a light-hole exciton; for $B>B_c$, the fundamental optical transition is a heavy-hole exciton. The value of B_c depends on the value of the relative valence-band offset, and a measurement of B_c can therefore directly provide information about q_v^0. We estimate $5\%<q_v^0<10\%$.

In Fig. 11 we reported the band structure for $\varepsilon_{Zn_{1-x}Mn_xSe}=-0.55\%$ and $q_v^0=5\%$ at zero magnetic field. The band structure is type I for light holes, and due to the strain effects is type II for heavy holes. Note that, in spite of the type-II character of the band structure, the oscillator strength of the heavy-hole transitions (Fig. 2) seems to be of the same order of magnitude as the oscillator strength of the light hole transitions. In fact, as can be seen in Fig. 12, the Coulombic interaction is responsible for the formation of interface excitons,[16,18] that is to say that the density of probability for the heavy holes is important near the interfaces. Moreover, from Fig. 12 it becomes clear that the magnetic-field-induced transition which occurs at the critical magnetic field B_c is a transition from a type-I light-hole exciton (for $B<B_c$) to a type-II heavy-hole exciton (for $B>B_c$).

The dependence on the magnetic field of the photoluminescences lines (Fig. 3) and the heavy hole lines observed in the excitation spectra of Fig. 4 is in agreement with the previous interpretation. The redshift of the σ^+ component of X^W_{HH} and X^T_{HH} is of the same order of magnitude as the one for the (Zn,Mn)Se photoluminescence line PL_B [Fig. 3(a)]. In particular, the redshift of the $PL_{T'}$ line (the σ^+ component of X^T_{HH}), which is observed up to 1.5 T, is quite parallel to the redshift of PL_B (Fig. 3). The magnetic field reinforces the type-II character of the band structure for the $-\frac{3}{2}$ spin component of the heavy holes, and the behavior of $X^T_{HH}(\sigma^+)$ confirms the large penetration of the $-\frac{3}{2}$ spin component heavy-hole wave function in (Zn,Mn)Se, as shown in Fig. 12. Note that no evidence of the magnetic-field-induced transition can be clearly observed in the magnetic-field dependence of the photoluminescence line (PL_T) energy in Fig. 3. Several reasons can be put forward. First, it can be seen in Fig. 10(a) that, above the critical magnetic field (that is to say above 3.5 T), the magnetic-field dependence of the $X^T_{HH}(\sigma^+)$ line begins to saturate. Second, around the transition, peaks $X^T_{HH}(\sigma^+)$ and $X^T_{LH}(\sigma^+)$ are close to each other [Fig. 10(a)] and are not resolved up to 5 T due to the width of the lines. The same phenomenon occurs in the photoluminescence spectrum, the full width at half maximum of the PL_T line being about 17 meV. In fact a mean value of the heavy- and light-hole exciton energies is measured in the photoluminescence spectra. Third, the photoluminescence measurements involve extrinsic characteristics such as excitons bound on defects or impurities. So it has been chosen to demonstrate the existence of the magnetic-field-induced transition exclusively on the excitation measurements, which are more reliable because they involve intrinsic characteristics.

Finally, note the behavior of the σ^- component of X^T_{HH}, which is detailed in Fig. 4(a). Up to $B=1$ T, the σ^+ and σ^- variation energies are symmetric, as for a type-II structure. For $B>1$ T, however, $X^T_{HH}(\sigma^-)$ remains practically constant, as in the case of a type-I structure. In fact, the effect of the magnetic field is to transform the type-II structure in a type-I structure for the $+\frac{3}{2}$ spin component of the heavy hole (see Fig. 12).

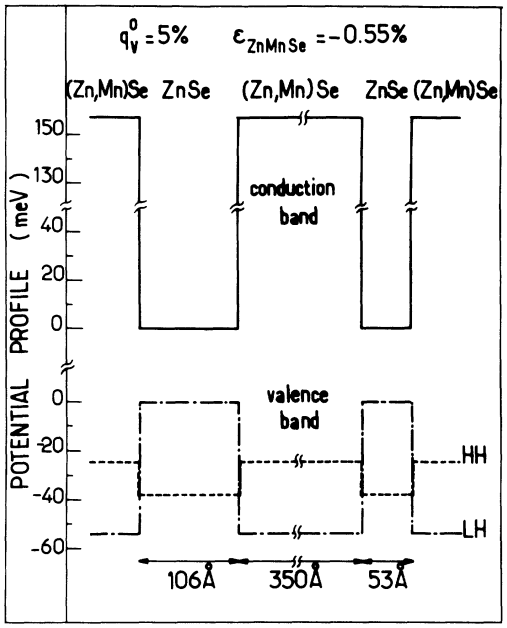

FIG. 11. Calculated potential profile along the growth axis of the heterostructure taking into account the strain effects on the band structure. The strain-free relative valence-band offset is taken as $q_v^0=5\%$, the strain in (Zn,Mn)Se layers is taken $\varepsilon_{Zn_{1-x}Mn_xSe}=-0.55\%$.

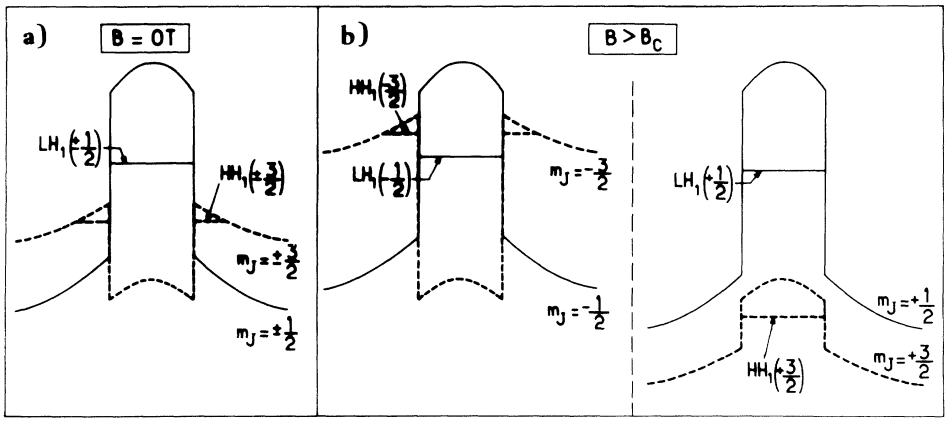

FIG. 12. Schematized potential experienced by the holes taking into account the Coulomb interaction for two different magnetic fields: (a) $B=0$ T and (b) $B > B_c$. The energy levels are also reported for the different spin components of the light and heavy holes.

For $\varepsilon_{Zn_{1-x}Mn_xSe}=-0.55\%$ and $q_v^0=10\%$ this transition is calculated at 1.4 T.

The excitation spectra of the wide well versus the magnetic field [Fig. 4(b)] do not show a crossing between the X_{LH}^W line and the $X_{HH}^W(\sigma^+)$ line as do the excitation spectra of the thin well. In fact, such a transition is expected at a higher critical magnetic field (about 5 T at $T=4.2$ K). The dependence of the critical magnetic field on the thickness of the well can be understood by looking at the valence band schematized in Fig. 12(a). For a large well the energy difference between the light- and heavy-hole transitions at zero magnetic field is increased. This is due to the decrease of the confinement energy of the light hole and to the fact that the interface exciton binding energy of the type-II heavy-hole exciton is smaller for a wide well than for a thin well (the overlap between the electronic and heavy-hole wave functions is smaller).

B. Time-resolved experiments

Let us now consider time-resolved measurements. In fact, the smaller overlap of the electron and hole wave functions in a type-II exciton compared to a type-I exciton should cause an increase in radiative lifetime. The increase of the recombination time of the thin well with magnetic field seems to be correlated with the existence of the crossing between the X_{LH}^T and $X_{HH}^T(\sigma^+)$ lines, since for the wide well no such crossing and also no variation of the recombination time are observed. Moreover the onset of the plateau observed in the magnetic-field dependence of the photoluminescence decay time of the thin well occurs at 2.5 T (for $T=4.2$ K), and the crossing the excitonic levels is calculated at 3 T (for $T=4.2$ K, $\varepsilon_{Zn_{1-x}Mn_xSe}=-0.55\%$ and $q_v^0=5\%$).

The observed recombination time of the type-I light-hole exciton of around 110 ps for low magnetic field is quite consistent with the usual values obtained for type-I structures such as GaAs/(Ga,Al)As (Ref. 24) or CdTe/(Cd,Mn)Te.[25,26] On the contrary, typical type-II recombination times are 1–10 ns,[27] whereas the experimental values saturate above $B=2.5$ T at about $\tau=240$ ps. This latter value is rather coherent with characteristic times of nonradiative processes.[28]

We therefore conclude that nonradiative processes, which are faster than radiative ones, dominate the recombination of the type-II excitons at high magnetic fields, thereby hiding to a certain extent the large increase of the radiative lifetime. Nevertheless, assuming a constant value for τ_{NR} ($\tau_{NR}\approx 240$ ps), the observed rise of the overall recombination time τ by a factor of 2 originates from a large rise in τ_R [according to Eq. (1)] and confirms the idea of a magnetic-field-induced type-I to type-II transition. Moreover, at $T=10$ K in Fig. 7(a), we find that the higher value of the recombination time is reached for a higher magnetic field ($B_c\approx 4$ T) than for $T=1.7$ or 4.2 K ($B_c\approx 2.5$ T). In fact, the Zeeman effect decreases drastically when the temperature increases because of the $B/(T+T_0)$ term in the expression of the Brillouin function [Eq. (7)] reducing the redshift of the $X_{HH}^T(\sigma^+)$ line. As a consequence, the crossing between X_{LH}^T and $X_{HH}^T(\sigma^+)$ will occur at a higher magnetic field; this crossing is calculated at 2.7, 3.3, and 3.8 T for 1.7, 4.2, and 10 K, respectively, in good agreement with experimental findings. In the wide well, the fundamental optical transition remains a type-I light-hole exciton transition for the applied magnetic fields and for all three temperatures, with therefore a constantly short recombination time [Fig. 7(b)].

V. CONCLUSION

In summary, we have shown how the dependence on magnetic field of the fundamental and excited optical transition energies in heterostructures like ZnSe/(Zn,Mn)Se which contain a semimagnetic compound can provide precise and clear information about the nature of these transitions: a low magnetic-field variation is the signature of a light-hole transition and/or of a wave function which does not penetrate in the semimagnetic layer; a large magnetic-field variation indicates a heavy-hole transition and/or a wave function which is largely localized in the semimagnetic layer.

From a comparison between theoretical calculations (which take into account the strain effect, the Zeeman effect, the excitonic effect, and the diamagnetism of the exciton) and experiments, we find that, due to the strain

effect, the fundamental transition at zero magnetic field involves a type-I light-hole exciton, while the first excited optical transition is a type-II heavy-hole exciton. We show that a magnetic-field-induced transition in the nature of the excitonic fundamental transition of a 53-Å ZnSe quantum well occurs for a critical magnetic field $B_C = 3$ T. The value of B_C provides a measurement of the relative valence-band offset which is found to be $5\% < q_v^0 < 10\%$. Moreover, time-resolved experiments show the transition at B_C from a type-I exciton to a type-II exciton.

This whole study shows that a fundamental transition involving a light-hole exciton with large oscillator strength and a heavy-hole-like in-plane density of states can be obtained in such structures. The application of a magnetic field allows the tailoring of the wave functions.

ACKNOWLEDGMENTS

The Laboratoire de Physique de la Matière Condensée de l'Ecole Normale Supérieure is Laboratoire associé au Centre National de la Recherche Scientifique, aux Universités Paris 6 et Paris 7. One of us (B.O.) acknowledges support of Deutscher Akademischer Austrauschdienst. This work was also supported by Direction des Recherches-Etudes et Techniques grant 91164.

*Present address: 3M Company, 3M Center, St. Paul, MN 55144-100.

[1]M. Haase, J. Qiu, J. De Puydt, and H. Cheng, Appl. Phys. Lett. **59**, 1272 (1991).

[2]A. Twardowski, T. Dietl, and N. Demianiuk, Solid State Commun. **48**, 845 (1983).

[3]X. Liu, A. Petrou, J. Warnock, B. T. Jonker, G. A. Prinz, and J. J. Krebs, Phys. Rev. Lett. **63**, 2280 (1989).

[4]B. T. Jonker, X. Liu, W. C. Chou, A. Petrou, J. Warnock, J. J. Krebs, and G. A. Prinz, J. Appl. Phys. **69**, 6097 (1991); X. C. Liu, W. C. Chou, A. Petrou, J. Warnock, B. T. Jonker, G. A. Prinz, and J. J. Krebs, in *Proceedings of the 20th International Conference on the Physics of Semiconductors,* edited by E. M. Anasassakis and J. D. Joannopoulos (World Scientific, Singapore, 1991), Vol. 1, p. 621.

[5]R. B. Bylsma, J. Kossut, W. M. Becker, L. A. Kolodziejski, R. L. Gunshor, and R. Frohne, J. Appl. Phys. **61**, 3011 (1987).

[6]W. Heimbrodt, O. Goede, Th. Köpp, R. Enderlein, M. Pessa, and J. Lilja, J. Cryst. Growth **101**, 705 (1990); Ma Ke-Jun and W. Giriat, Solid State Commun. **60**, 927 (1986).

[7]H. Luo, N. Dai, F. C. Zhang, N. Samarth, M. Dobrowolska, J. K. Furdyna, C. Parks, and A. K. Ramdas, Phys. Rev. Lett. **70**, 1307 (1993).

[8]J. A. Gaj, J. Ginter, and R. R. Galazka, Phys. Status Solidi B **89**, 655 (1978).

[9]H. Hillmer, A. Forchel, T. Kuhn, G. Mahler, and H. P. Meier, Phys. Rev. B **43**, 13 992 (1992).

[10]F. H. Pollak and M. Cardona, Phys. Rev. **172**, 816 (1968).

[11]Y. Merle d'Aubigné, H. Mariette, N. Magnea, H. Tuffigo, R. T. Cox, G. Lentz, Le Si Dang, J. L. Pautrat, and A. Wasiela, J. Cryst. Growth **101**, 650 (1990); H. Mathieu, J. Allère, and G. Gil, Phys. Rev. B **4**, 2218 (1991).

[12]A. Blacha, H. Presting, and M. Cardona, Phys. Status Solidi B **126**, 11 (1984).

[13]D. Wasik, Z. Liro, and M. Baj, J. Cryst. Growth **101**, 466 (1990).

[14]I. Berlincourt, H. Jaffe, and L. R. Shiozawa, Phys. Rev. **129**, 1009 (1963).

[15]L. A. Kolodziesjki, S. Sakamoto, R. L. Gunshor, and S. Datta, Appl. Phys. Lett. **44**, 799 (1984).

[16]E. Deleporte, J. M. Berroir, C. Delalande, N. Magnea, H. Mariette, J. Allègre, and J. Calatayud, Phys. Rev. B **45**, 6305 (1992).

[17]E. Deleporte, J. M. Berroir, G. Bastard, C. Delalande, J. M. Hong, and L. L. Chang, Phys. Rev. B **42**, 5891 (1990); G. Peter, E. Deleporte, J. M. Berroir, C. Delalande, J. M. Hong, and L. L. Chang, *ibid.* **44**, 11 302 (1991).

[18]G. Peter, E. Deleporte, G. Bastard, J. M. Berroir, C. Delalande, B. Gil, J. M. Hong, and L. L. Chang, J. Lumin. **52**, 147 (1992).

[19]I. Strzalkowski, S. Joshi, and C. R. Corwell, Appl. Phys. Lett. **28**, 350 (1976).

[20]Author, in *Title,* edited by O. Madelung and M. Schulz, Landolt-Börnstein, New Series, Group X, Vol. IV, Part 22a (Springer, Berlin, 1987).

[21]Y. Hefetz, J. Nakahara, A. V. Nurmikko, L. A. Kolodziejski, R. L. Gunshor, and S. Datta, Appl. Phys. Lett. **47**, 989 (1985).

[22]J. E. Potts, H. Cheng, S. Mohapatra, and T. L. Smith, J. Appl. Phys. **61**, 333 (1987).

[23]L. A. Kolodziejski, R. L. Gunshor, T. C. Bonsett, R. Venkatasubramanian, S. Datta, R. B. Bylsma, W. M. Becker, and N. Otsuka, Appl. Phys. Lett. **47**, 169 (1985).

[24]J. Martinez-Pastor, A. Vinattieri, L. Carraresi, M. Colocci, Ph. Roussignol, and G. Weimann, Phys. Rev. B **47**, 10 456 (1993); A. Pohlmann, R. Helmann, E. O. Göbel, D. R. Yakovlev, W. Ossau, A. Waag, R. N. Bicknell-Tassius, and G. Landwehr, Appl. Phys. Lett. **61**, 2929 (1992).

[25]Ph. Roussignol, J. Martinez-Pastor, A. Vinattieri, E. Deleporte, C. Delalande, M. Colocci, and B. Lunn, Phys. Rev. B **48**, 11 871 (1993).

[26]Y. Hefetz, W. C. Goltsos, A. V. Nurmikko, L. A. Kolodziesjki, and R. L. Gunshor, Appl. Phys. Lett. **48**, 372 (1986).

[27]R. Ferreira, P. Rolland, Ph. Roussignol, C. Delalande, A. Vinattieri, L. Carraresi, M. Colocci, N. Roy, B. Sermage, J. F. Palmier, and B. Etienne, Phys. Rev. B **45**, 11 782 (1992).

[28]M. Gunoli, A. Vinattieri, M. Colocci, C. Deparis, J. Massies, G. Neu, A. Bosacchi, and S. Franchi, Phys. Rev. B **44**, 3115 (1991).